

Electrochemical synthesis of SnO₂ films containing three-dimensionally organized uniform mesopores *via* interfacial surfactant templating†

Ryan L. Spray and Kyoung-Shin Choi*

Received (in Berkeley, CA, USA) 23rd March 2007, Accepted 25th July 2007

First published as an Advance Article on the web 8th August 2007

DOI: 10.1039/b704428c

SnO₂ films containing organized mesopores and nanocrystalline frameworks with easily removable surfactant templates were produced electrochemically using interfacial amphiphilic assemblies formed on the working electrode as a template.

SnO₂ has many technological applications including photoelectrochemical cells, gas sensing, and rechargeable Li-ion batteries.¹ The efficiencies of these devices directly rely on the surface areas and interfacial structures of film-type SnO₂ electrodes. Therefore, many efforts have been made to produce mesoporous SnO₂ with enhanced surface areas and interfacial kinetics.² If the mesoporous structure is composed of *uniform* pore size and pore connections, it can also offer opportunities to study the effect of specific nanostructural details on chemical and physical properties of the SnO₂ electrodes. In addition, charge transport properties of uniformly organized mesoporous frameworks are reported to be superior to those of mesoporous films composed of randomly connected nanoparticles creating unorganized mesoscale voids.³ Therefore, achieving the synthetic ability to produce SnO₂ or other inorganic films with various organized mesoporous structures (*i.e.* connectivity, pore size) can be highly desirable for both fundamental studies and technological applications.

To date, SnO₂ with organized mesoporous structures has been prepared *via* precipitation or sol-gel based methods combined with supramolecular surfactant templating.² However, most of these syntheses were aimed to prepare *powder*-type materials that cannot be readily integrated into electrochemical devices. Successful production of high quality mesoporous SnO₂ *films* by sol-gel based dip-coating methods has been relatively limited. This is probably because the sol-gel based dip-coating method involves synthetic variables that may not be freely controlled (*e.g.* rate of evaporation, rate of hydrolysis).

In this study, we report an electrochemical interfacial surfactant templating method that provides a one-step procedure to construct SnO₂ films containing organized mesopores and nanocrystalline frameworks with easily removable surfactant templates. In this method, surfactant templates were organized by surface forces at the solid/liquid interface (*i.e.* the working electrode surface) and construction of inorganic frameworks was achieved by electrodeposition. This is quite different from the sol-gel dip coating method where surfactant self-assemblies are induced by evaporation and inorganic mesoporous walls are produced by the sol-gel

processes. Therefore, this method can provide a general complementary route to the sol-gel dip-coating method for producing SnO₂ and other various materials as mesoporous films. The electrochemical interfacial templating method has been previously used to produce films with two dimensional mesoporous structures (*e.g.* lamellar and 2D hexagonal),⁴ but this is the first time to produce films containing a three-dimensional mesoporous structure by this method.

SnO₂ films were electrodeposited by reduction of NO₃⁻ ions, which generates OH⁻ ions (NO₃⁻ + H₂O + 2e⁻ → NO₂⁻ + 2OH⁻; E° = 0.01 V vs. NHE).⁵ An increase in the local pH near the working electrodes provides for deposition of SnO₂ as a film on the working electrode. A typical plating medium used for this synthesis contains 0.1 M SnCl₂, 0.4 M HNO₃ and 0.5 M NaNO₃ (See ESI† for detailed experimental conditions).

In order to introduce a mesoporous structure into SnO₂ films, 2 wt% of anionic surfactant, sodium dodecyl sulfate (SDS), was added to the plating medium as a structure directing agent. Self-assembly of amphiphilic molecules at the solid/liquid interface is a well known phenomenon although it has not been methodically exploited to construct inorganic mesoporous films.⁶ When the SDS molecules form interfacial layers on the working electrode by surface forces, Sn⁴⁺ ions join the surface of interfacial SDS micelles serving as counter ions to minimize the repulsion between the anionic head groups (Fig. 1). As a result, well-organized arrangement of Sn⁴⁺ ions can be achieved on the working electrode by the presence of interfacial SDS assemblies. The types of amphiphilic structures stabilized on the working electrode depend on the nature of the substrate (*e.g.* surface charge density, hydrophilicity, external bias) as well as the composition of the

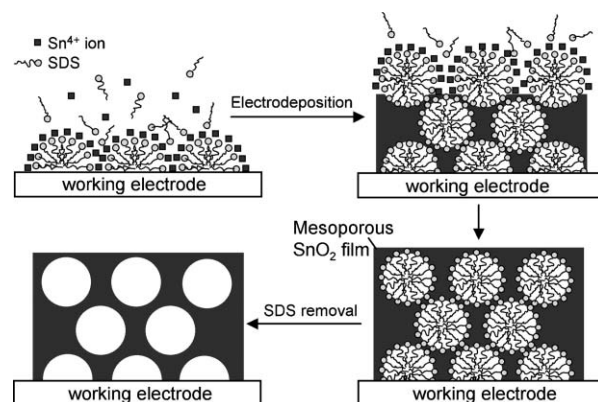


Fig. 1 Schematic representation of electrochemical interfacial surfactant templating.

Department of Chemistry, Purdue University, West Lafayette, IN, 47907, USA. E-mail: kchoi1@purdue.edu; Fax: 1-765-494-0239; Tel: 1-765-494-0049

† Electronic supplementary information (ESI) available: Experimental details; SEM images; XPS and EDS data of SnO₂ films before and after SDS removal. See DOI: 10.1039/b704428c

solution (e.g. type of surfactants, type and concentration of counter ions, pH).⁶

When electrodeposition initiates, this arrangement of Sn^{4+} ions around the SDS micelles directly becomes the skeleton of the SnO_2 films forming mesoporous frameworks (Fig. 1). As the film grows, additional amphiphilic layers continuously form on the new film surface maintaining the same mesostructure initially stabilized on the working electrode. This leads to the incorporation of a homogenous mesoporous structure throughout the film.⁴ The interfacial surfactant assemblies used as templates in this method can form even in an extremely dilute surfactant solution (<critical micelle concentration) and their structures are independent from the solution surfactant structures. Therefore, this approach is conceptually different from the previous electrochemical method using a lyotropic liquid crystalline phase of surfactants in a plating medium as a template.⁷

The X-ray diffraction (XRD) pattern of SnO_2 films deposited with 2 wt% of SDS shows (110) and (101) reflections of tetragonal SnO_2 structure ($P4_2/mnm$, JCPDS #41-1445) (Fig. 2(a)). The broadening of these reflections indicates the nanocrystalline nature of the SnO_2 films. The particle size obtained from XRD peak broadening using the Scherrer equation is approximately 1.5 nm. The small angle X-ray diffraction of the same film shows a well defined peak centered at $2\theta = 2.38^\circ$ and a broad second order peak centered at $2\theta = 4.78^\circ$. These peaks indicate the presence of organized mesoporous structures with an average repeating unit of ca. 3.7–3.8 nm (Fig. 2(b)).

The scanning electron micrograph (SEM) shows the particulate nature of SnO_2 films composed of 50–150 nm spherical particles (ESI^\dagger). This is due to the multiple nucleation processes during electrodeposition. The transmission electron microscopy (TEM) study shows that each SnO_2 particle contains a well-defined

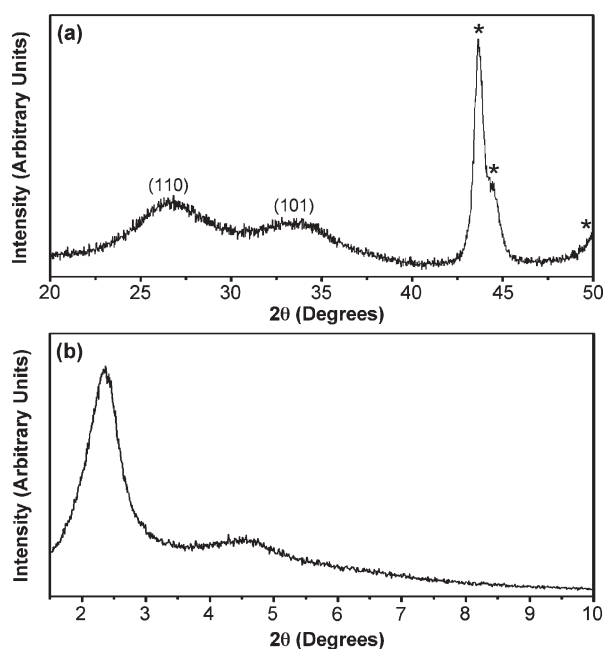


Fig. 2 (a) Wide angle and (b) small angle XRD patterns of SnO_2 films deposited with 2 wt% SDS. $\text{Cu-K}\alpha$ radiation is used for both measurements. Diffraction patterns created by a stainless steel working electrode are indicated by *.

worm-like mesoporous structure (Fig. 3(a)). The worm-like structure is best described as one-dimensional rod-type micelles entangled in a three-dimensional manner.⁸ As a result, this structure provides an isotropic porous structure with easily accessible pore openings from any directions, which makes this structure highly desirable for various electrochemical and photo-electrochemical applications.³ The TEM study also reveals that there are many domains with more regularly arranged pore channels in the worm-like structure (circled area in Fig. 3(a)), which is responsible for the appearance of the weak and broad second-order peak in the small-angle XRD pattern (Fig. 2(b)).

High-resolution TEM (HRTEM) images of the inorganic walls between the pores show atomic lattice fringes of SnO_2 , indicating that the as-deposited films already contain a nanocrystalline framework without the need for thermal treatment (Fig. 3(b)). This result agrees well with the line broadening in the wide-angle XRD pattern. Production of mesoporous films with crystalline walls can be highly beneficial for achieving superior charge transport properties as well as high surface areas than those with amorphous walls. However, production of crystalline mesoporous walls is not commonly achieved in sol-gel based synthesis without additional thermal treatments.

Construction of SnO_2 films with a worm-like structure using SDS- Sn^{4+} surface assemblies is the first example of producing a three-dimensional mesoporous structure *via* electrochemical interfacial surfactant templating. Previous studies showed that SDS formed exclusively bilayer interfacial assemblies with divalent ions (Zn^{2+} and Ni^{2+}) regardless of SDS concentrations, resulting in construction of two-dimensional lamellar structures.⁴ The fact that SDS- Sn^{4+} surface assembly does not adopt a lamellar structure indicates that the charge of the metal counter ions (tetravalent tin ions *vs.* divalent zinc or nickel ions) is one of the major factors that affect the interfacial packing patterns of SDS.⁹ This result also implies that this method has the potential to create more diverse mesoporous structures (e.g. three-dimensional gyroid or micellar cubic mesoporous structures) when factors that govern the stability of interfacial structures during electrodeposition are further investigated.

In order to utilize surface areas enhanced by porous structures, removing surfactants without collapsing the mesoporous framework is crucial. In this electrochemical method, the surfactant molecules do not become the part of the inorganic wall structure; the electrostatic interactions between Sn^{4+} and the sulfate head groups of SDS during electrodeposition disappear when Sn^{4+} ions are deposited as neutral SnO_2 , which leaves SDS merely

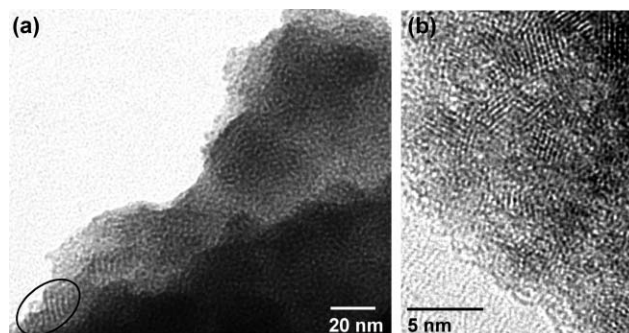


Fig. 3 (a) TEM and (b) HRTEM images of the mesoporous SnO_2 film.

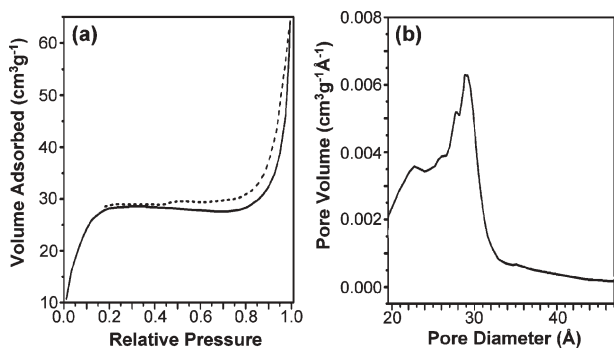


Fig. 4 (a) Nitrogen adsorption (—) and desorption (---) isotherm for mesoporous SnO₂ film; (b) pore size distribution determined by Horvath-Kawazoe analysis of the adsorption isotherm branch.

physisorbed on the surface of SnO₂ deposits. This made it possible to remove SDS from the pores by simply soaking the films in deionized water for 9–12 hours (or 6 hours with gentle stirring). The absence of SDS in the films was confirmed by X-ray photoelectron spectroscopy (XPS) and energy dispersive X-ray spectroscopy (EDS) (ESI†). The fact that SDS can be easily removed by a solution process also indicates the accessibility of the pores in the SnO₂ films. The SnO₂ film after SDS removal showed an identical small angle XRD pattern to that shown in Fig. 2(b), indicating that the SnO₂ mesoporous walls remained intact during the surfactant dissolution process.

After SDS was removed, the porosity of the SnO₂ film was characterized by N₂ adsorption/desorption analysis. N₂ adsorption/desorption analysis for mesoporous films is often not reported because it calls for a relatively large quantity of materials (>100 mg), which requires scaling up the synthesis without affecting the quality of the mesostructure. The method described here can produce films as thick as 20 microns while maintaining the uniformity of the mesostructure, allowing for relatively facile sample preparation for N₂ adsorption/desorption analysis. The SnO₂ films exhibited a type IV isotherm with H₃-type hysteresis, confirming the mesoporous features of the film (Fig. 4(a)).¹⁰ The mean pore size, pore volume and Brunauer-Emmett-Teller (BET) surface area of sample are 28 Å, 0.113 cm³ g⁻¹, and 163 m² g⁻¹ (or 1133 m² cm⁻³), respectively (Fig. 4(b)).

The photoelectrochemical property of the mesoporous SnO₂ films was characterized by measuring the zero-bias (short circuit) and potential-dependent photocurrent (Fig. 5). The SnO₂ films were heated at 100 °C for 1 h before the photocurrent measurement to ensure good adhesion between the SnO₂ particles and the conducting substrate that may have been loosened during the soaking process for SDS removal. The SnO₂ films generate anodic photocurrent under irradiation, which is a typical behavior for an n-type semiconductor. Both the nanocrystallinity and thin mesoporous walls of the SnO₂ films contribute to the generation of well-defined photocurrent; more efficient charge transport processes are expected in nanocrystalline walls than amorphous walls and the mesoporous structure significantly reduces the distance for the photon-generated holes to travel to the SnO₂/electrolyte interface. These features decrease the rate of electron-hole recombination considerably and enhance the photocurrent.

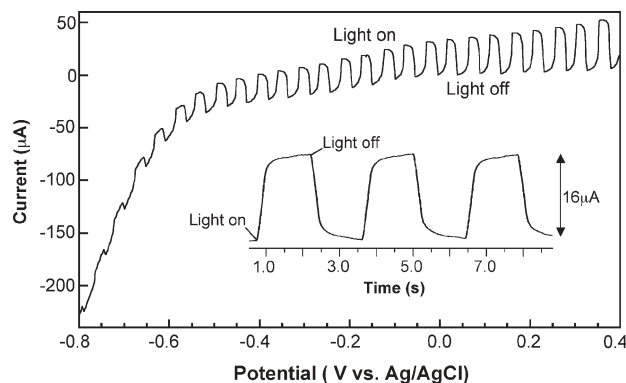


Fig. 5 Current-voltage characteristics for a mesoporous SnO₂ film using chopped irradiation (scan rate = 50 mV s⁻¹). The inset shows photocurrent versus time measured at zero-bias. A 300 W Xe lamp with the incident light flux of 2.5 W cm⁻² was used as the light source and a 0.1 M sodium acetate solution was used as an electrolyte (pH 9.0).

Annealing the SnO₂ films higher than 100 °C did not improve photocurrent, indicating that the as-deposited SnO₂ films already possess optimum nanocrystallinity. These mesoporous SnO₂ films are currently being investigated for use in dye-sensitized solar cells and gas sensors.

This work made use of the Life Science and the Birk Microscopy Facilities at Purdue University, and was financially supported by the U.S. Department of Energy (DE-FG02-05ER15752) and the Alfred P. Sloan Research Foundation. We thank Professor Eric Stach and Mr Seng Min Kim for their help in obtaining HRTEM images.

Notes and references

- 1 A. Kay and M. Grätzel, *Chem. Mater.*, 2002, **14**, 2930; T. Bedja, S. Hotchandani and P. V. Kamat, *J. Phys. Chem.*, 1994, **98**, 4133; N. Barsan, M. Schweizer-Berberich and W. Göpel, *Fresenius' J. Anal. Chem.*, 1999, **365**, 287; J.-M. Tarascon and M. Aramand, *Nature*, 2001, **414**, 359.
- 2 P. Yang, D. Zhao, D. I. Margolese, B. F. Chmelka and G. D. Stucky, *Nature*, 1998, **396**, 152; K. G. Severin, T. M. Abdel-Fattah and T. J. Pinnavaia, *Chem. Commun.*, 1998, 1471; N. Ulagappan and C. N. R. Rao, *Chem. Commun.*, 1996, 1685; J. Ba, J. Polleux, M. Antonietti and M. Niederberger, *Adv. Mater.*, 2005, **17**, 2509.
- 3 M. Zúkalová, A. Zúkal, L. Kavan, M. K. Nazeeruddin, P. Liska and M. Grätzel, *Nano Lett.*, 2005, **5**, 1789.
- 4 Y. Tan, E. M. P. Steinmiller and K.-S. Choi, *Langmuir*, 2005, **21**, 9618; Y. Tan, S. Srinivasan and K.-S. Choi, *J. Am. Chem. Soc.*, 2005, **127**, 3596.
- 5 G. H. A. Therese and P. V. Kamath, *Chem. Mater.*, 2000, **12**, 1195.
- 6 J.-F. Liu and W. A. Ducker, *J. Phys. Chem. B*, 1999, **103**, 8558; I. Burgess, C. A. Jeffrey, X. Cai, G. Szymanski, Z. Galus and J. Lipkowski, *Langmuir*, 1999, **15**, 2607.
- 7 G. S. Attard, P. N. Bartlett, N. R. B. Coleman, J. M. Elliot, J. R. Owen and J. H. Wang, *Science*, 1997, **278**, 838.
- 8 M. E. Cates and S. J. Candau, *J. Phys.: Condens. Matter*, 1990, **2**, 6869.
- 9 A. Khan, B. Jönsson and H. Wennerström, *J. Phys. Chem.*, 1985, **89**, 5180; D. Maciejewska, A. Khan and B. Lindman, *Colloid Polym. Sci.*, 1986, **264**, 909; E. J. Wanless and W. A. Ducker, *Langmuir*, 1997, **13**, 5418.
- 10 F. Rouquerol, J. Rouquerol and K. Sing, in *Adsorption by Powders and Porous Solids: Principles, Methodology and Applications*, Academic Press, London, 1999.